Research Square

Preprints are preliminary reports that have not undergone peer review.
They should not be considered conclusive, used to inform clinical practice,
or referenced by the media as validated information.

Dielectric Analysis of BFO/PVDF Nanocomposites as a Function of Frequency and Filler Concentration

Sukhvir Singh
MSJ College
Reshu Khandelwal
MSJ College
Ravi Kumari
MSJ College
Dinesh Kumar Yadav
University of Rajasthan
Harish Kumar Meena
S S Jain Subodh P.G. College
Balram Tripathi
S S Jain Subodh P.G. College
Anju Tanwar
tanwaranjumsjc@gmail.com

MSJ College

Research Article

Keywords: $BiFeO_3$, polyvinylidene fluoride, nanocomposite, solution casting

Posted Date: November 25th, 2026

DOI: https://doi.org/10.21203/rs.3.rs-11160261/v1

License: This work is licensed under a Creative Commons Attribution 4.0 International License.
Read Full License

Additional Declarations: No competing interests reported.

Dielectric Analysis of BFO/PVDF Nanocomposites as a Function of Frequency and Filler Concentration

Sukhvir Singh[1], Reshu Khandelwal[1], Ravi Kumari[1], Dinesh Kumar Yadav [2] , Harish Kumar Meena[3], Balram Tripathi[3], Anju Tanwar[1*]

[1] *Department of Physics, M.S.J. College, Bharatpur, Rajastha, India - 321001*

[2]*Department of Physics, University of Rajasthan, Jaipur, Rajasthan, India -302004*

[3]*S.S. Jain Subodh P.G. (Auto.) College, Rambagh, Jaipur, Rajasthan, India -302004*

[*]*tanwaranjumsjc@gmail.com*

This study used the solution casting approach to successfully fabricate flexible $BiFeO_3$ (BFO)/ polyvinylidene fluoride (PVDF) nanocomposite films containing 1–5 wt% of BFO. To illuminate the influence of BFO inclusion on the structural, molecular, morphological, and dielectric attributes of the polymer matrix PVDF, BFO/PVDF nanocomposites are analyzed. X-ray diffraction (XRD), scanning electron microscopy (SEM), and Fourier-transform infrared (FTIR) spectroscopy are employed to characterize composites formed by incorporating BFO nanoparticles into PVDF at various filler concentrations. Measurements of frequency-dependent dielectric done to study the dielectric properties of synthesized nanocomposites. Sol-gel method was used to create BFO nanoparticles and subsequently calcined at 650°C. Crystalline rhombohedral perovskite structure of BFO was verified via XRD analysis. FT-IR analysis revealed concentration-dependent changes in local vibrational environment of PVDF. SEM observations revealed progressive changes in composite morphology as the BFO content increased, indicating an expansion of heterogeneous ceramic-polymer interfacial region. Dielectric measurements clearly demonstrated that the response was dependent on both concentration and frequency. Relative permittivity increased from approximately 3.07 for 1 wt% BFO to 32.28 for 5 wt% BFO at low-frequency end. Within same concentration range, low-frequency dielectric loss tangent increased from approximately 0.070 to 0.339. Relative permittivity decreased with increasing frequency, whereas loss tangent decreased initially and showed a subsequent increase at higher frequencies for several compositions. Through combined effects of ceramic polarization, filler-polymer interfacial interactions, and heterogeneous interfacial polarization, incorporation of BFO successfully modulates the dielectric response of PVDF—as evidenced by structural, molecular, morphological, and dielectric results. Thus, within measured frequency range, these composites could be regarded as adjustable dielectric materials.

Keywords: $BiFeO_3$; polyvinylidene fluoride; nanocomposite; solution casting; dielectric permittivity; dielectric loss.

Abbreviations

- BFO — Bismuth Ferrite ($BiFeO_3$)
- DMF — N,N-Dimethylformamide
- FTIR— Fourier-Transform Infrared Spectroscopy
- MWS — Maxwell-Wagner-Sillars (Interfacial polarization)
- PVDF — Polyvinylidene fluoride
- SEM — Scanning Electron Microscopy
- Wt% — Weight Percentage
- XRD — X-Ray Diffraction

1 . Introduction

The requirement for dielectric substances that combine high energy storage capacity with great mechanical flexibility[1] and simplicity of manufacturing has increased due to the rising need for wearable sensors, flexible electronics. Polyvinylidene fluoride (PVDF)[2] and its copolymers have garnered lot of interest among polymer-based dielectric materials because of their exceptional mechanical strength, superior chemical stability, and high dielectric breakdown strength. The polymorphic semi-crystalline fluoropolymer PVDF can crystallize into five distinct phases: α, β, γ, δ, and ε.[4–8] Under typical melt or solution processing conditions, PVDF frequently crystallizes into the non-polar α-phase. because this phase has a trans-gauche (TGTG) chain structure and is thermodynamically the most stable. to its maximum net dipole moment per unit cell, which results in excellent electroactive, ferroelectric, and piezoelectric performance, the highly polar β-phase with an all-trans (TTTT) conformation of PVDF is especially favored for dielectric[9] and energy harvesting applications.[8, 10, 11] Because of its low intrinsic dielectric[12] constant (ε_r < 10 at 1 kHz), efficiency and immaculate PVDF potential energy storage density are severely limited in capacitive applications.[4, 13] One of the most successful techniques to boost dielectric permittivity of pristine polymers is the production of ceramic polymer nanocomposites, in which high-permittivity inorganic ceramic nanoparticles are scattered throughout a continuous and flexible polymer matrix.[5, 14] Due to its remarkable multifunctional properties, multiferroic[15] bismuth ferrite (BFO)[16, 17] has drawn a lot of scientific interest among the several advanced ceramic fillers investigated for polymer nanocomposites. BFO is a rhombohedrally deformed perovskite having R3c symmetry in its crystal structure[18] This material is characterized by the coexistence of G-type antiferromagnetism and ferroelectricity, both of which endure much above \room temperature.[16, 19–21] The high leakage current, intrinsic brittleness, and substantial dielectric loss of pure BFO ceramics limit their practical usage in capacitor applications[22], despite their appealing functional qualities.[23–27] These restrictions are mostly related to the loss of bismuth ions during high-temperature solid-state synthesis, which causes oxygen vacancies to develop and negatively impact BFO electrical characteristics. A practical strategy to get past these intrinsic problems is to embed BFO nanoparticles in a highly resistant PVDF matrix. While PVDF matrix acts as an insulating barrier that reduces long-range charge conduction and improves dielectric breakdown resistance, the final composite benefits from the high permittivity of BFO.[14, 28–30] There are two main reasons why BFO/PVDF nanocomposites have an increased dielectric constant. One of the primary reasons of Maxwell-Wagner-Sillars (MWS) interfacial polarization is the substantial mismatch in electrical conductivity and dielectric permittivity

between the semiconducting BFO nanoparticles and the highly insulating PVDF matrix.[5, 6, 31, 32] Mobile charge carriers move in the direction of the polymer–ceramic interfaces when exposed to an alternating electric field. The concentration of these carriers causes substantial interfacial polarization, which is most noticeable at low frequencies. Second, BFO nanoparticles promote nucleation within the PVDF matrix, facilitating the crystallization process. The –CH_2/–CF_2 dipoles seen in the PVDF macromolecular chains interact electrostatically with the locally charged BFO nanoparticle surfaces.[7, 33] By encouraging PVDF chains to change from the all-trans conformation to the thermodynamically stable α-phase, these interfacial interactions minimize the requirement for mechanical stretching and enable the in-situ generation of the electroactive β-phase.[7, 34–38]

Although ceramic fillers have better characteristics, their high surface energy makes it difficult to ensure their equal distribution throughout the polymer matrix.[6, 23] Van der Waals interactions encourage nanoparticle agglomeration at high filler loadings, leading to microstructural porosity and localized electric field distortions. By creating interconnecting electrical channels, the agglomeration of ceramic nanoparticles promotes localized electron hopping, which lowers breakdown strength and increases dielectric loss.[39, 40]

Thus, understanding the relationship between BFO loading, dielectric permittivity, and dielectric loss is important for assessing the dielectric performance of BFO/PVDF nanocomposites.[14, 41] Additionally, the three-dimensional Nanoparticle dispersion inside the polymer matrix is influenced by the geometric constriction imposed by the film thickness.[42] The thickness-dependent dielectric response of BFO/PVDF nanocomposites has not, however, been thoroughly studied.[43] To address this research gap, the present study investigates flexible BFO/PVDF nanocomposite films containing 1–5 wt% BFO nanoparticles, fabricated using the solution-casting technique. It provides a detailed assessment of filler dispersion, Maxwell-Wagner-Sillars (MWS) interfacial polarization, and dielectric behavior in relation to filler content. The findings offer guidelines for designing low-loss BFO/PVDF nanocomposites for flexible energy storage applications and elucidate how varying the filler weight percentage influences dielectric performance.

2. Material and Methods

***2.1. Materials*:** Alfa Aesar, USA, supplied poly (vinylidene fluoride) (PVDF) powder (CAS No. 24937-79-9, melting point 155–160°C). Because of its remarkable mechanical flexibility, great chemical stability, high dielectric breakdown strength, and exceptional inherent ferroelectric and piezoelectric capabilities, PVDF, a semi-crystalline fluoropolymer, was carefully chosen as the foundation polymer matrix. Because of these qualities, it is a perfect matrix option for creating sophisticated flexible dielectric nanocomposites. The organic solvent used was N,N-Dimethylformamide (DMF) (analytical reagent grade, purity ≥99.0%, CAS No. 68-12-2), which was acquired from Central Drug House (CDH), India. BFO nanoparticles were created by a straightforward and affordable sol-gel method. Following synthesis and drying, the BFO precursor was synthesized, dried, and then calcined for one hour at 650°C before being cooled to room temperature. XRD was used to evaluate the crystalline phase of the calcined powder. and subsequently cooled; this

process removes moisture and facilitates the formation of phases detectable by XRD. Notably, this calcination method suppresses the formation of thermodynamically stable impurity phases while promoting the crystallization of BFO nanoparticles into a high-quality, single-phase, perovskite structure with a rhombohedral distortion (part of the R3c space group).

2.2 BFO/PVDF Nanocomposite Film Preparation or Synthesis

BFO/PVDF nanocomposite films were created using the traditional solution-casting technique. To prepare a clear and homogeneous solution. First, DMF was used to dissolve PVDF powder. During this process, the mixture was continuously stirred magnetically at 250 rpm and a temperature of 45°C for two hours until the PVDF had completely dissolved and formed a transparent solution. To prevent particle agglomeration and ensure a stable suspension, calcined BFO nanoparticles were added to DMF in varying amounts (In relation to the total mass of the BFO/PVDF solid components, the BFO concentrations of 1,2,3 & 5 wt.% were computed.) and ultrasonicated for 30 minutes. Subsequently, With constant magnetic stirring, the ultrasonicated BFO suspension was gradually added to the PVDF solution. The resultant mixture was agitated at 400 rpm for six hours and then ultrasonically treated for thirty minutes to guaranty that the ceramic nanoparticles were evenly distributed throughout the polymer matrix. After that, the mixture was transferred into a sterile glass Petri dish, heated to 60°C in a hot-air oven for 48 hours, and allowed to dry until the DMF had evaporated. The completely dried films were removed from the glass substrate and kept in a desiccator before being characterized.

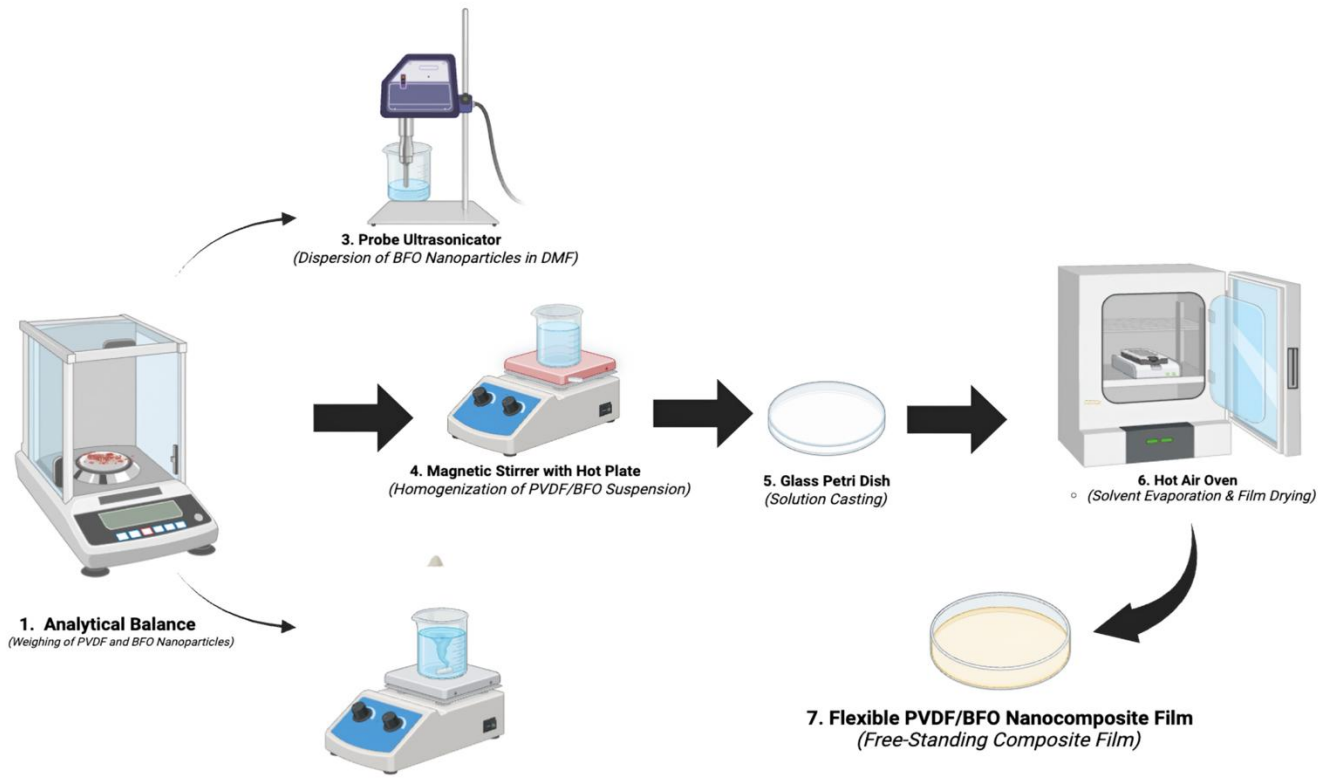


Figure 1: Fabrication of BFO/PVDF nanocomposite films

2.3. Characterization of BFO/PVDF nanocomposites

A Rigaku Miniflex-600 diffractometer set to 20 kilovolts and 20 milliamperes with Cu Kα radiation (λ = 1.5418 Å) was used to obtain XRD spectra of the manufactured composites. Diffraction angle patterns between 5° and 60° were collected using a scan speed of 10° per minute and a sample width of 0.02°. FT-IR (SHIMADZU, IRSpirit) was employed in the wavenumber range of 3000–500 cm-1 with a resolution of 4 cm-1 and 45 scans per sample at room temperature to investigate potential interactions between BFO and PVDF as well as functional groups. A scanning electron microscope (Carl Zeiss, EVO 18) equipped with energy-dispersive X-ray spectroscopy (EDX) at various resolutions and magnifications was used to record the surface morphology and distribution of Filler (BFO) particles in PVDF. Samples were covered with a thin layer of conducting material before to examination in order to enhance image quality. An impedance analyzer (WAYNE KERR-6500B, West Sussex, UK) was used to investigate the frequency-dependent dielectric properties of the BFO–PVDF nanocomposite films at room temperature. The dielectric loss tangent (tan{\delta}) and relative dielectric constant (\epsilonr) were computed as a function of frequency for each of the different BFO loadings.

RESULT AND DISCUSSION

3.1 *X-ray Diffraction analysis*

Figure 2 Shows the XRD patterns of pristine PVDF, synthetic BFO nanoparticles, and BFO/PVDF composite films containing 1, 3, and 5 wt.% BFO. The crystal structure, phase properties, and structural morphology of virgin PVDF, the produced BFO nanoparticles, and the resulting BFO/PVDF nanocomposites were all carefully examined using XRD. The (020), (110), and (021) crystalline planes of the monoclinic α-phase polymorph are represented by distinctive diffraction reflections in the XRD pattern of the Pristine PVDF matrix at roughly 2θ = 18.3°, 19.8°, and 26.4°. The distinct and well-defined diffraction peaks found at 2θ ≈ 22.56°, 31.90°, 32.20°, 39.64°, 45.92°, 51.46°, 57.14°, and 67.20° for the synthesized BFO nanoparticles correspond to the (012), (104), (110), (006), (214), and (220) planes. Upon incorporating BFO nanoparticles into the PVDF matrix, the characteristic reflections associated with the polymer host and the ceramic filler are retained in the nanocomposites. This indicates the successful formation of the BFO/PVDF composite network without structural degradation or phase decomposition of either component. A distinct alteration is observed in the primary diffraction signature of PVDF within the composite sample, where standard reflections shift or merge to form a clear reflection at 2θ = 20.1°, A change in the pristine PVDF-(110), and (021) crystallographic planes of the monoclinic α-phase related diffraction feature is observed near 2θ ≈ 20.1° after BFO incorporation,

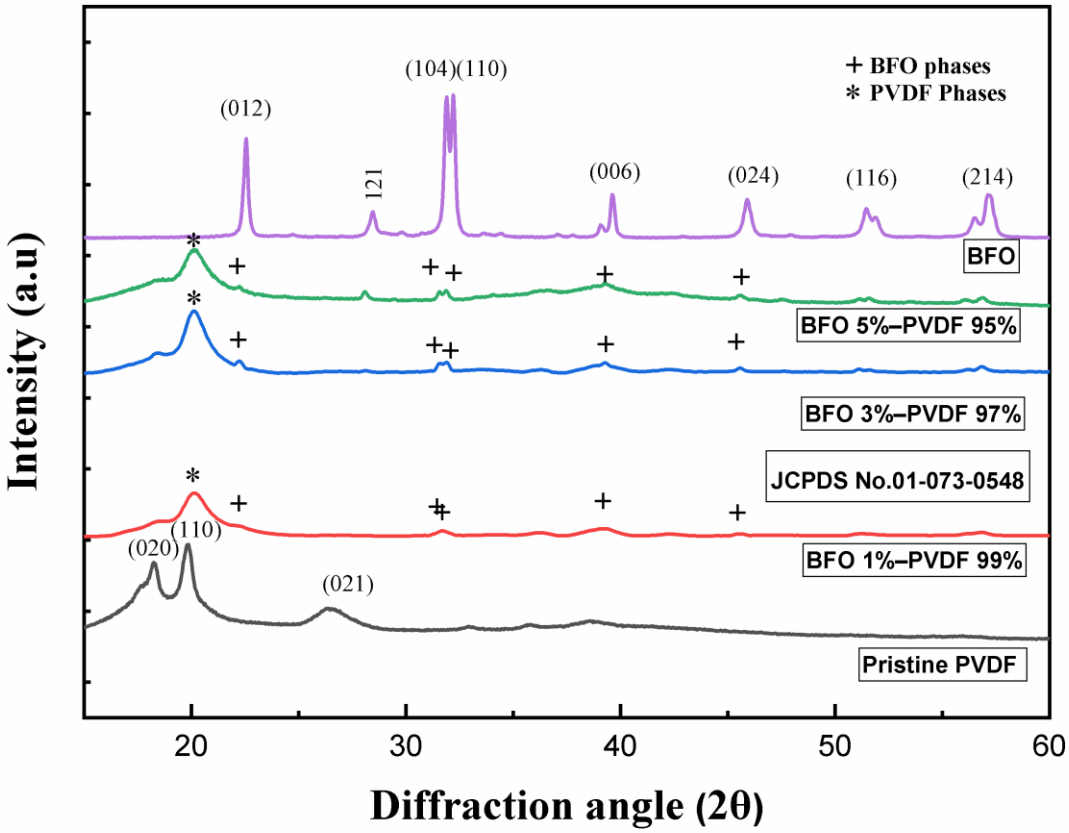


Figure 2: X-ray diffraction patterns of pristine PVDF, BFO, and BFO/PVDF composites.

indicating a modification of the crystalline diffraction profile of PVDF. The '+' signs in Figure 2 illustrate how reflections associated with the BFO phase become more distinct and easily identifiable with higher filler content. Overall, the XRD results confirm the coexistence of the crystalline BFO phase and the PVDF matrix, demonstrating that the incorporation of filler is essential for controlling the polymorphic properties of the polymer matrix.

Lattice Parameters and Crystallite Size

The indexed XRD reflections were used to assess the lattice parameters and crystallite size of the produced BFO phase. According to the rhombohedrally distorted perovskite structure of $BiFeO_3$ (JCPDS No. 01-073-0548), the diffraction peaks at 22.56° 31.90°, 32.20°, 39.64°, 45.92°, 51.46°, 57.14°, and 67.20°. The characteristic rhombohedral distortion of the BFO lattice is demonstrated by the distinct splitting of the reflections near 32° into the (104) and (110) components. Lattice parameters were calculated using the interplanar spacing obtained from Bragg's law. Based on the hexagonal representation of the rhombohedral R3c structure, The lattice parameters were found to be a = b = 5.571 Å and c = 13.728 Å. The estimated unit-cell volume was 368.99 Å^3. These values closely match the reported crystallographic parameters for rhombohedral BFO.

The Scherrer equation,

$$D = \frac{K\lambda}{\beta \cos\theta}$$

Table 1 : Structural parameters of BFO nanoparticles obtained from XRD analysis, including diffraction angle (2θ), interplanar spacing (d), FWHM, and apparent crystallite size (D)

Plane (hkl)	$2\theta(°)$	d (Å)	FWHM (°)	Apparent crystallite size, D (nm)
(012)	22.56	3.938	0.240	33.81
(104)	31.90	2.803	0.245	33.69
(110)	32.20	2.778	0.228	36.24
(006)	39.64	2.272	0.216	39.01
(024)	45.92	1.975	0.396	21.77
(116)	51.46	1.774	0.315	27.99
(214)	57.14	1.611	0.400	22.63

where λ = 1.5406 Å is the wavelength of Cu Kα radiation, K = 0.9 is the form factor, θ is the Bragg angle, and β is the full width at half maximum (FWHM) of the diffraction peak in radians. Based on the chosen reflections, the average apparent crystallite size was 30.4 ± 6.3 nm, with a range of 21.8 to 39.0 nm. These numbers should be considered apparent crystallite sizes since instrumental broadening was not adjusted.

Phase Evolution and Structural Modification

The crystalline structure of the polymer composite changes noticeably when BFO is added to the PVDF matrix. At roughly 2θ = 18.26°, 19.84°, and 26.36°, Pristine PVDF exhibits its characteristic diffraction reflections, which correspond to the (020), (110), and (021) planes, respectively. The primary PVDF-related diffraction feature moves toward roughly 2θ=20.14° upon BFO introduction, indicating a change in the PVDF matrix's crystalline environment. BFO-related reflections are also visible in the composite patterns, especially around 22.5°, 32.5°, 39.6° and 45.9°. These reflections become more noticeable as BFO loading increases. These findings suggest that upon composite formation, the crystalline BFO phase is preserved inside the PVDF matrix. The primary PVDF-related reflection shifts toward roughly 2θ = 20.14°, indicating that BFO addition alters the PVDF crystalline diffraction profile. This change implies that the PVDF matrix's crystalline environment has changed. Overall, the XRD data show that BFO inclusion preserves the distinctive crystalline phase of BFO while altering the crystalline structure of PVDF.

FT-IR spectroscopy:

FTIR spectra were examined to determine characteristic vibrational bands associated with the functional groups present in the samples. The molecular-level vibrational properties of PVDF and associated BFO/PVDF nanocomposites were investigated using FT-IR spectroscopy. Their characteristic profiles are shown in Figure 3. The wavenumber range of 500–3000 cm^{-1} was used to acquire infrared spectra. Distinct absorption bands appear in the pristine PVDF at approximately 770, 959, 1083, and 1293 cm^{-1}. Interestingly, the band typically observed at 763–766 cm^{-1}—traditionally connected to the non-polar α-phase of PVDF—closely resembles the vibrational band found at approximately 770 cm^{-1}. The internal vibrations of the PVDF macromolecular backbone and the localized bending/stretching modes of the CH_2/CF_2 groups are responsible for the remaining absorption peaks. Upon the addition of 1 wt% BFO, the main absorption bands appear at approximately 774, 964, 1087, and 1297 cm^{-1}. The presence of BFO nanoparticles alters the local vibrational environment of the host polymer chains; this is evident from a systematic shift of approximately 4–5 cm^{-1} compared to pristine PVDF. As the BFO filler content is increased to 3 and 5 wt%, the infrared absorption profiles undergo gradual changes. Key bands in these profiles are observed at approximately 872–868, 1166–1161, 1398–1392, and 1678–1666 cm^{-1}. The host polymer matrix's molecular environment is

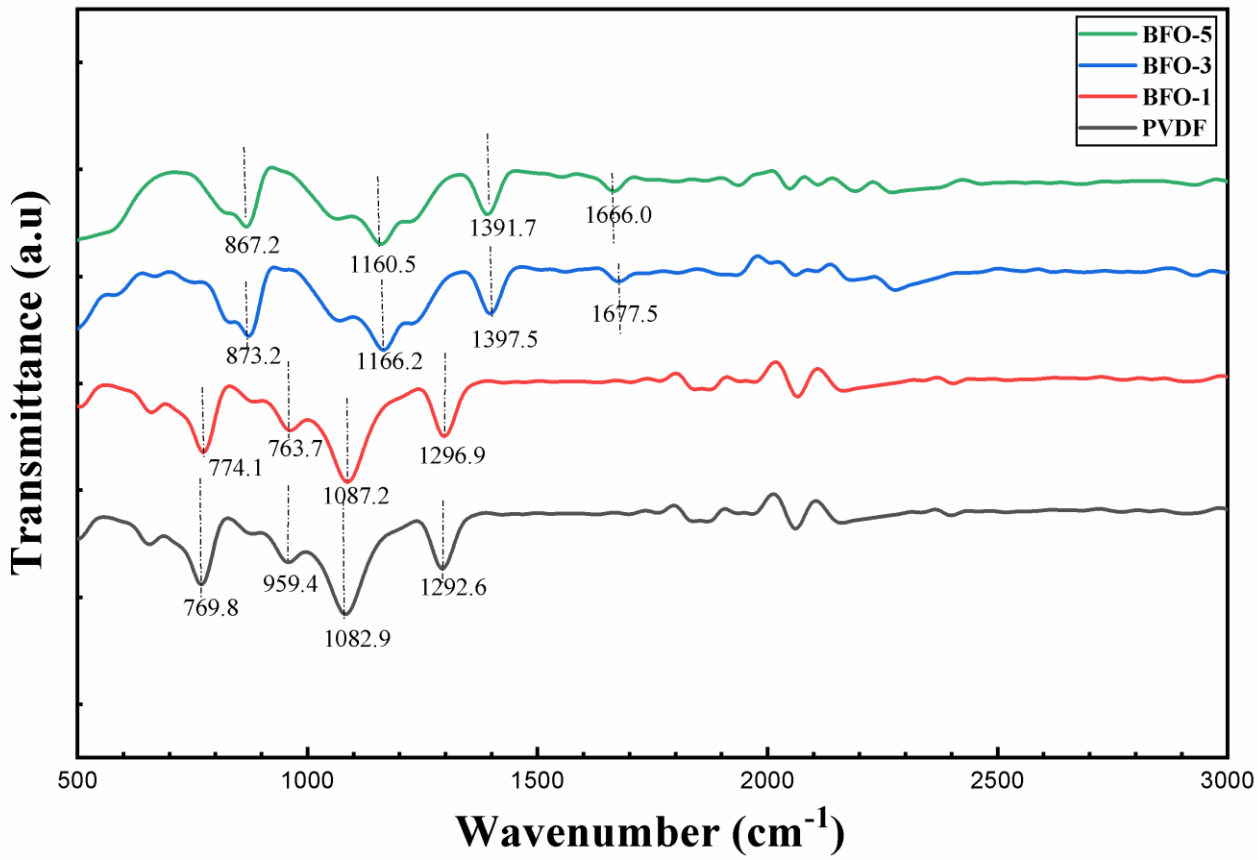


Figure 3 :FTIR spectra of pristine PVDF and BFO/PVDF nanocomposites

systematically altered by the addition of ceramic nanoparticles. as indicated by the concentration-dependent changes in band positions and the overall spectral profile. Interestingly, The characteristic vibrational response of the PVDF matrix remains observable after BFO incorporation, although noticeable changes in peak position, intensity, and spectral profile occur with increasing BFO loading indicating that the structural integrity of the main PVDF backbone remains unaffected. Interfacial molecular interactions at the boundaries The observed spectrum shifts are caused by interactions between the BFO fillers and the surrounding PVDF chains. The current experimental data do not conclusively indicate the formation of covalent BFO/PVDF bonds, although similar studies on BFO/PVDF composites have reported spectral shifts in the 400–800 cm^{-1} range, attributed to filler-matrix coupling[44]. Therefore, rather than the formation of new chemical bonds, these spectral shifts are attributed to interfacial or molecular physical interactions. These vibrational results align with the XRD findings. XRD analysis reveals that the addition of BFO alters the crystalline structure of PVDF; similarly, FTIR profiles indicate corresponding changes in the local molecular vibrational environment. The observed dielectric response of the BFO–PVDF composite may be influenced by these structural and interfacial changes, particularly those related to interfacial polarization.

3.4 Surface morphology:

The surface appearance and microstructural features of the synthesized BFO and BFO/PVDF composite samples were examined using scanning electron microscopy (SEM). Figures 4(a–c) display the SEM micrographs of BFO, BFO 1%–PVDF 99%, and BFO 5%–PVDF 95%. SEM images of the BFO powder reveal a highly diverse and non-uniform morphology, featuring angular, fractured, and irregularly shaped particles of varying sizes. The morphology

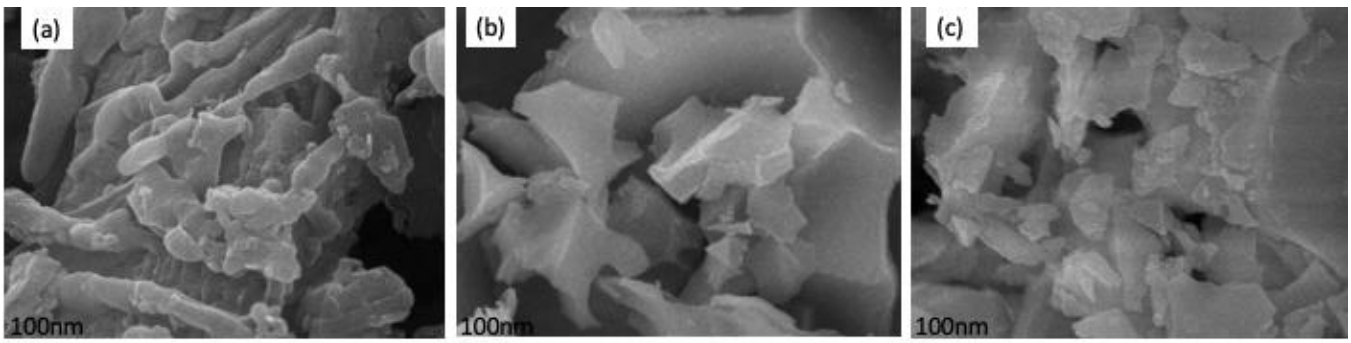


Figure 4:SEM micrographs of (a) BFO, (b) BFO 1%–PVDF 99%, and (c) BFO 5%–PVDF 95%.

that appears suggest that the produced BFO material is made up of particles. Distinct changes in morphology are observed upon incorporating BFO into the PVDF matrix. In the BFO (1%)–PVDF (99%) composite, irregular flake- or plate-like structures appear within the polymeric matrix, alongside regions where the morphology is relatively compact. When the BFO content is increased to 5 wt%, the microstructure appears more heterogeneous, characterized by a higher density of closely packed and overlapping particles or flake-like structures. As the filler content increases, the presence of irregularly

shaped BFO-containing regions becomes even more pronounced. These morphological changes indicate that increasing the BFO content alters the microstructural arrangement of the PVDF matrix and the filler-polymer interface. The SEM data aligns with the XRD and FTIR results, indicating that the incorporation of BFO induces structural and molecular changes within the PVDF matrix. As the fraction of the inorganic BFO phase increases, the additional interfaces formed within the polymer matrix can influence charge accumulation and interfacial polarization under an electric field. Consequently, the morphological changes observed with increasing BFO content can affect the composite's dielectric response (which is dependent on the loading.

4. Impedance spectroscopy:

4.1 Dielectric Constant

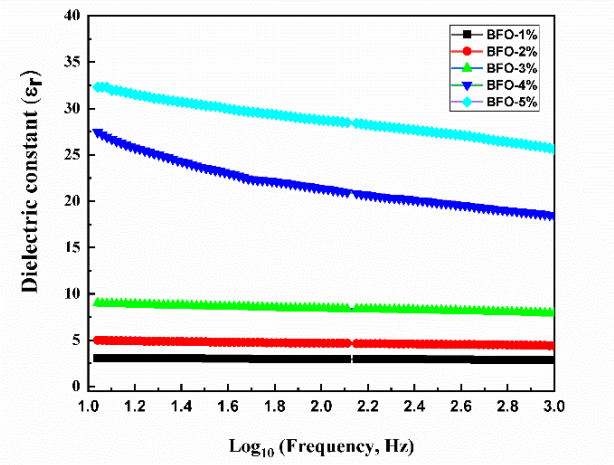


Figure 5: Frequency dependence of the dielectric constant of BFO–PVDF composites.

The dielectric constant was found to consistently drop with increasing frequency for all BFO concentrations. Within the examined low-frequency range, the dielectric constant rises from approximately 3.07 for the BFO 1%–PVDF 99% composite to 4.99, 9.01, 27.42, and 32.28 for the BFO 2%–PVDF 98%, BFO 3%–PVDF 97%, BFO 4%–PVDF 96%, and BFO 5%–PVDF 95% composites, respectively. In the high-frequency range, these dielectric constant values decrease to approximately 2.85, 4.41, 7.93, 18.44, and 25.60. Consequently, the dielectric response depends significantly on both frequency and BFO concentration, with the 5 wt% BFO composites exhibiting the highest dielectric constant. Frequency-dependent polarization processes are responsible for the BFO/PVDF system's apparent reduction in ϵ_r with increasing frequency. When frequencies are low, Because slow polarization processes, like interfacial and space-charge polarization, have enough time to react to the applied electric field, the dielectric constant is comparatively high. As the frequency increases, Because these sluggish polarization processes are unable to keep up with the quickly shifting electric field, the dielectric constant gradually drops. The significant increase in ϵ_r observed with rising BFO content is attributed to the combined effect of the polarizable BFO phase and the increased contact areas between BFO and PVDF. Charge collection at the filler-polymer interface is made easier by the dielectric mismatch between the ceramic BFO filler and the PVDF matrix, which increases interfacial polarization and raises the dielectric response overall.

At low frequencies, the 5 wt.% BFO/PVDF composite exhibits a notably high dielectric constant (approximately 32.28), indicating that the incorporation of higher BFO content significantly improves the composite's polarization capability. Dielectric behavior dependent on both content and frequency has also been observed in the BFO/PVDF composite system. For the 5 wt% BFO composites, the dielectric constant decreased from approximately 32.28 to 25.60 as the frequency increased, indicating the significance of slow polarization processes at low frequencies. Furthermore, structural and morphological changes revealed by XRD, FTIR, and SEM analyses are associated with variations dependent on this concentration. The incorporation of BFO alters the crystalline and molecular environment of the PVDF matrix and creates more heterogeneous interfaces, which can facilitate interfacial charge accumulation. Thus, the combined effects of BFO incorporation, interfacial polarization, and structural/morphological changes induced by the filler within the PVDF matrix may be responsible for the enhanced dielectric response of the BFO–PVDF composite.

Table 2 :Representative dielectric constant values of BFO–PVDF composites at different frequencies.

$\log_{10}(f)$	Frequency (Hz)	BFO-1%	BFO-2%	BFO-3%	BFO-4%	BFO-5%
1.0404	10.98	3.06496	4.98576	9.01272	27.42168	**32.27960**
1.5051	31.99	3.02022	4.82596	8.69312	23.55452	**30.29808**
2.0101	102.35	2.96908	4.66616	8.43744	21.34928	**28.73204**
2.4950	312.57	2.92754	4.57028	8.21372	19.84716	**27.38972**
3.0000	1000.00	2.85083	4.41048	7.92608	18.44092	**25.59996**

Dielectric loss:

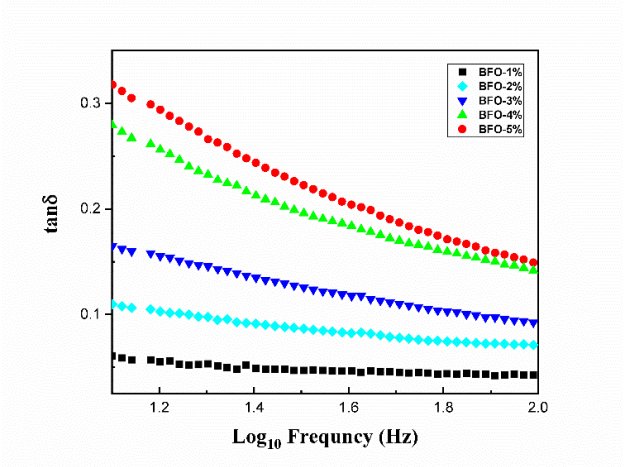


Figure 6: Frequency dependence of the dielectric loss tangent ($tan\,\delta$) of BFO/PVDF composites with different BFO loadings at room temperature.

Figure 6 represent the frequency-dependent tan δ of the BFO/PVDF composites. Both the frequency and the BFO filler content have a major impact on the dielectric loss. The dielectric loss increases systematically with increasing BFO content in the low- frequency region of the investigated range; in particular, the $tan\,\delta$ values for composites containing 1%, 2%, 3%, 4%, and 5% BFO are roughly 0.070,

0.116, 0.174, 0.299, and 0.339, respectively. Dielectric loss thus increases significantly with higher BFO additions, particularly in the low-frequency band. The rise in dielectric loss with increasing BFO concentration is caused by the increased role of interfacial polarization and charge buildup at the BFO/PVDF interface. The number and effective area of BFO/PVDF interfaces increase as the ceramic filler content rises, offering more locations for charge accumulation when an electric field is present. Therefore, increased interfacial polarization and the resulting energy loss may be the cause of the higher dielectric loss seen with higher BFO content. Additionally, local charge displacement may be facilitated by the unique microstructure created by the addition of BFO, which would explain the observed rise in dielectric loss. All compositions exhibit a distinct frequency dependence. Dielectric loss first decreases with increasing frequency, indicating that comparatively sluggish polarization processes (such space-charge and interfacial polarization) are the main source of contribution at lower frequencies. There is less dielectric loss at higher frequencies because these sluggish charge-displacement processes are unable to keep up with the quickly shifting electric field. The onset of faster localized polarization or charge-transport processes may be the cause of the slight increase in several compositions that follows the minimum loss value at intermediate frequencies. While the inclusion of BFO improves the composite's overall polarizability, it also results in higher dielectric loss, as evidenced by the simultaneous increases in the dielectric constant and dielectric loss with increasing BFO content. This behavior reflects the inherent trade-off between increased dielectric capability and energy loss in heterogeneous polymer-ceramic systems. Among the composites examined, the 5 weight percent BFO composites showed the strongest polarization response, as evidenced by the highest dielectric constant and low-frequency dielectric loss. As a result, choosing the ideal BFO concentration for a particular dielectric application necessitates striking a balance between the allowable degree of dielectric loss and the required dielectric permittivity.

CONCLUSION:

The impact of adding BFO nanoparticles[45] on structural characteristics, morphology, and dielectric behavior was successfully investigated using BFO-filled PVDF nanocomposites. XRD investigation revealed distinctive reflections that corresponded to a rhombohedrally deformed perovskite structure, confirming the crystalline nature of the produced BFO phase. The local molecular environment of the PVDF matrix is changed by the addition of BFO, according to FTIR measurements. Increasing the BFO content changes the microstructural arrangement of the PVDF matrix, and SEM measurements show that BFO has an uneven particle structure. An extensive and unique BFO/PVDF interfacial area forms as filler content increases, offering more sites for charge buildup and interfacial polarization. These structural changes align with the concentration- and frequency-dependent dielectric[46] behavior of the composite. The dielectric measurements showed a clear increase in the relative dielectric constant as the BFO level rose. The dielectric constant rose from roughly 3.07 for the BFO 1%–PVDF 99% composition to 32.28 for the BFO 5%–PVDF 95% composition in the low-

frequency range of the examined range, indicating a roughly 10.5-fold increase throughout the composite series. Due to slow interfacial and space-charge polarization processes that could not keep pace with the applied alternating electric field, the dielectric constant decreased with increasing frequency for all compositions. In the low-frequency range, dielectric loss increased alongside the BFO concentration; specifically, the tanδ value rose from approximately 0.070 for the 1 wt% composite to 0.339 for the 5 wt% composite. This concurrent rise in dielectric loss and dielectric constant suggests that although improved BFO/PVDF interfacial polarization increases the polarizability of the composite, it also results in increased energy loss. Given that the 5 weight percent BFO composite has both the greatest dielectric loss and the highest dielectric permittivity, the highest measured permittivity should be chosen based on the particular needs of the dielectric application. Combined results from XRD, FTIR, SEM, and dielectric measurements indicate that the incorporation of BFO alters the morphology, crystal structure, local molecular environment, and interfacial polarization behavior of the PVDF matrix. The XRD and FTIR results show no evidence of the complete destruction of the PVDF structure or the formation of a new crystalline chemical phase[48] within the composite system. Therefore, structural modifications induced by the filler, BFO/PVDF interfacial polarization, and the intrinsic polarization contribution of BFO are the primary factors driving the enhanced dielectric response. These results show the potential of BFO/PVDF nanocomposites as adjustable dielectric materials and emphasize the trade-off between dielectric permittivity and dielectric loss as the ceramic filler percentage increases.

Acknowledgements:

One of the authors expresses his sincere gratitude to the Government of India's University Grants Commission (UGC) for its financial assistance through the Junior Research Fellowship (JRF). The facilities for X-ray diffraction (XRD), Fourier-transform infrared (FTIR) spectroscopy & dielectric measurements were provided by S.S. Jain Subodh P.G. (Autonomous) College, Jaipur, and IIT Jodhpur provided the scanning electron microscopy (SEM) facility, for which the authors are very grateful. The authors would like to express their sincere gratitude to all the institutions and facilities that provided invaluable assistance in completing the characterization work reported in this study.

ORCID

Sukhvir Singh https://orcid.org/0009-0007-9920-9291

Reshu Khandelwal https://orcid.org/0009-0003-9529-8718

Ravi Kumari https://orcid.org/0009-0008-6441-0312

Anju Tanwar https://orcid.org/my-orcid?orcid=0000-0003-4956-1450

Balram Tripathi https://orcid.org/0000-0002-8324-7863

Harish Kumar Meena https://orcid.org/0000-0002-4280-3077

Dinesh Kumar Yadav https://orcid.org/0000-0002-8306-6480

References

1. Tanwar A (2023) Study of Free Volume in Polymer Blends by PALS. Eur Chem Bull 2023, Vol 12, Special Issue 5, Page 1403–1406 12(Special Issue 5):1403–1406. https://doi.org/10.48047/ecb/2023.12.si5a.016.
2. Dallaev R, Pisarenko T, Sobola D, Orudzhev F, Ramazanov S, Trčka T (2022) Brief Review of PVDF Properties and Applications Potential. Polymers 2022, Vol 14, Page 4793 14:4793
3. Concha VOC, Timóteo L, Duarte LAN, Bahú JO, Munoz FL, Silva AP, Lodi L, Severino P, León-Pulido J, Souto EB (2024) Properties, characterization and biomedical applications of polyvinylidene fluoride (PVDF): a review. Journal of Materials Science 2024 59:31 59:14185–14204
4. Saxena P, Shukla P (2021) A comprehensive review on fundamental properties and applications of poly(vinylidene fluoride) (PVDF). Adv Compos Hybrid Mater 4:8–26
5. Yuan J, Yao S, Poulin P (2016) Dielectric constant of polymer composites and the routes to high-k or low-k nanocomposite materials. In: Polymer Nanocomposites: Electrical and Thermal Properties. Springer International Publishing, pp 3–28
6. Singh M, Apata IE, Samant S, Wu W, Tawade B V., Pradhan N, Raghavan D, Karim A (2021) Nanoscale Strategies to Enhance the Energy Storage Capacity of Polymeric Dielectric Capacitors: Review of Recent Advances. Polymer Reviews 62:211–260
7. Petrukhin D, Salnikov V, Nikitin A, … IS-J of C, 2024 undefined Effect of Bismuth Ferrite Nanoparticles on Physicochemical Properties of Polyvinylidene Fluoride-Based Nanocomposites. mdpi.comD Petrukhin, V Salnikov, A Nikitin, I Sidane, S Slimani, S Alberti, D Peddis, A OmelyanchikJournal of Composites Science, 2024•mdpi.com
8. Mohammadpourfazeli S, Arash S, Ansari A, Yang S, Mallick K, Bagherzadeh R (2023) Future prospects and recent developments of polyvinylidene fluoride (PVDF) piezoelectric polymer; fabrication methods, structure, and electro-mechanical properties. RSC Adv 13:370–387
9. Xia W, Zhang Z (2018) PVDF-based dielectric polymers and their applications in electronic materials. IET Nanodielectrics 1:17–31
10. Costa CM, Cardoso VF, Martins P, et al (2023) Smart and Multifunctional Materials Based on Electroactive Poly(vinylidene fluoride): Recent Advances and Opportunities in Sensors, Actuators, Energy, Environmental, and Biomedical Applications. Chem Rev 123:11392–11487
11. Costa CM, Cardoso VF, Martins P, et al (2023) Smart and Multifunctional Materials Based on Electroactive Poly(vinylidene fluoride): Recent Advances and Opportunities in Sensors, Actuators, Energy, Environmental, and Biomedical Applications. Chem Rev 123:11392–11487
12. Rawat A, Mahavar HK, Tanwar A, Singh PJ (2014) Dielectric relaxation studies of polyvinylpyrrolidone (PVP) and polyvinylbutyral (PVB) in benzene solutions at microwave frequency. Indian J Pure Appl Phys 2014, Vol 52, Page 632–636 52(9):632–636.
13. Moharana S, Mishra MK, Chopkar M, Mahaling RN (2016) Enhanced dielectric properties of surface hydroxylated bismuth ferrite–Poly (vinylidene fluoride-co-hexafluoropropylene) composites for energy storage devices. Journal of Science: Advanced Materials and Devices 1:461–467
14. Yadav NP, Sahu BB, Mahaling RN, Yadav T, Tripathi PK, Moharana S (2023) Superior dielectric and electrical characteristics of poly(methylmethacrylate) (PMMA)-BiFeO3-Polystyrene-2% divinyl benzene (PDB) composites. Optik (Stuttg) 277:170695
15. Kharbanda S, Dhanda N, Aidan Sun AC, Thakur A, Thakur P (2023) Multiferroic perovskite bismuth ferrite nanostructures: A review on synthesis and applications. J Magn Magn Mater 572:170569
16. Mansingh RK, Mishra RK, Dash T (2021) Modifying BiFeO3(BFO) for multifunctional applications -a review. AIP Conf Proc. https://doi.org/10.1063/5.0072802/611288
17. Wu J, Fan Z, Xiao D, Zhu J, Wang J (2016) Multiferroic bismuth ferrite-based materials for multifunctional applications: Ceramic bulks, thin films and nanostructures. Prog Mater Sci 84:335–402
18. Meena HK, Meena K, Verma R, et al (2024) Tuning of Optical Properties via Annealing of Bismuth Ferrite (BiFeO3) Thin Films. Open Journal of Composite Materials 14:124–131

19. Wang N, Luo X, Han L, Zhang Z, Zhang R, Olin H, Yang Y (2020) Structure, Performance, and Application of BiFeO3 Nanomaterials. Nano-Micro Letters 2020 12:1 12:81-
20. Rhaman MM, Miah MS, Ahmad T (2024) Investigation of magnetic and electric properties of bismuth ferrite nanoparticles at different temperatures. Nano-Structures & Nano-Objects 39:101304
21. Ahmed I, Mustafa G, Umair Subhani M, Hussain G, Ismail AG, Anwar H (2022) A detailed investigation of lanthanum substituted bismuth ferrite for enhanced structural, optical, dielectric, magnetic and ferroelectric properties. Results Phys 38:105584
22. Nayak S, Agnihotri P, Nayak JP, Joshi C, Rai R (2025) Exploring bismuth ferrite: Structural changes and future applications. Current Applied Physics 73:49–76
23. Rutuparna Mahakhud RM, SheershaPradhan S, Krishna Satapathy KS (2025) A Review on Enhancement of Dielectric Loss and Constant of Bifeo3 and Different Type of Polymer Composites. International Journal of Engineering and Science Invention 14:40–43
24. Xie J, Xiao C, Shao S, Duan Q, Xie Q, Lü F (2021) Effect of Bismuth Ferrite Nanometer Filler Element Doping on the Surface Insulation Properties of Epoxy Resin Composites. Nanomaterials 2021, Vol 11, Page 2200 11:2200
25. Srivastava A, Singh AK, Srivastava ON, Tewari HS, Masood KB, Singh J (2020) Magnetic and Dielectric Properties of La and Ni Co-substituted BiFeO3 Nanoceramics. Front Phys 8:480348
26. Petrukhin D, Salnikov V, Nikitin A, Sidane I, Slimani S, Alberti S, Peddis D, Omelyanchik A, Rodionova V (2024) Effect of Bismuth Ferrite Nanoparticles on Physicochemical Properties of Polyvinylidene Fluoride-Based Nanocomposites. Journal of Composites Science 2024, Vol 8, Page 329 8:329
27. Peixoto MV, Costa FM, Devesa S, Graça MPF (2023) Structural, Morphological and Dielectric Characterization of BiFeO3 Fibers Grown by the LFZ Technique. Crystals 2023, Vol 13, Page 960 13:960
28. Cadenbach T, Benitez MJ, Morales AL, Vera CC, Lascano L, Quiroz F, Debut A, Vizuete K (2020) Nanocasting synthesis of BiFeO3 nanoparticles with enhanced visible-light photocatalytic activity. Beilstein Journal of Nanotechnology 11:164 11:1822–1833
29. You L, Liu B, Hua H, Jiang H, Yin C, Wen F (2023) Energy Storage Performance of Polymer-Based Dielectric Composites with Two-Dimensional Fillers. Nanomaterials 2023, Vol 13, Page 2842 13:2842
30. Sasmal A, Sen S, Devi PS (2020) Frequency dependent energy storage and dielectric performance of Ba–Zr Co-doped BiFeO3 loaded PVDF based mechanical energy harvesters: effect of corona poling. Soft Matter 16:8492–8505
31. Kum-onsa P, Chanlek N, Manyam J, Thongbai P, Harnchana V, Phromviyo N, Chindaprasirt P (2021) Gold-Nanoparticle-Deposited TiO2 Nanorod/Poly(Vinylidene Fluoride) Composites with Enhanced Dielectric Performance. Polymers 2021, Vol 13, Page 2064 13:2064
32. Kum-onsa P, Chanlek N, Manyam J, Thongbai P, Harnchana V, Phromviyo N, Chindaprasirt P (2021) Gold-Nanoparticle-Deposited TiO2 Nanorod/Poly(Vinylidene Fluoride) Composites with Enhanced Dielectric Performance. Polymers 2021, Vol 13, Page 2064 13:2064
33. Sasmal A, Patra A, Devi PS, Sen S (2021) Hydroxylated BiFeO3as efficient fillers in poly(vinylidene fluoride) for flexible dielectric, ferroelectric, energy storage and mechanical energy harvesting application. Dalton Transactions 50:1824–1837
34. Miyashita T, Saito H (2023) Crystal polymorphism of poly(vinylidene fluoride) blended with alkylammonium salts exhibiting different ion-dipole interaction strengths. Polymer Journal 2023 55:6 55:711–715
35. Wang Y, Lei D, Wu L, Ma R, Ning H, Hu N, Lee A (2023) Effects of stretching on phase transformation of PVDF and its copolymers: A review. Open Physics. https://doi.org/10.1515/PHYS-2022-0255/XML
36. Mireja S, Khakhar D V. (2024) High β-phase PVDF films formed by uniaxial compression. Polymer (Guildf) 293:126665
37. Dowarah S, Kalita P, Singh DP, Kumar S (2025) Formation and saturation of β-phase of PVDF in DMF solvent: a comprehensive study. Soft Mater 23:1–11

38. Concha VOC, Timóteo L, Duarte LAN, Bahú JO, Munoz FL, Silva AP, Lodi L, Severino P, León-Pulido J, Souto EB (2024) Properties, characterization and biomedical applications of polyvinylidene fluoride (PVDF): a review. Journal of Materials Science 2024 59:31 59:14185–14204
39. Adhlakha N, Yadav KL, Truccato M, Manjusha (2016) Reduced leakage current and improved multiferroic properties of 0.5((1−x)BLPFO-xPZT)-0.5PVDF composite films. Ceram Int 42:18238–18246
40. Xie Z, Liu D, Xiao Y, Wang K, Zhang Q, Wu K, Fu Q (2022) The effect of filler permittivity on the dielectric properties of polymer-based composites. Compos Sci Technol 222:109342
41. Bhadra D, Masud MG, Sarkar S, Sannigrahi J, De SK, Chaudhuri BK (2012) Synthesis of PVDF/BiFeO 3 nanocomposite and observation of enhanced electrical conductivity and low-loss dielectric permittivity at percolation threshold. J Polym Sci B Polym Phys 50:572–579
42. Zhao XF, Zhang XN, Yu M (2024) Multiscale understanding the interfacial layer in poly(vinylidene fluoride)-based ferroelectric polymers. Materialia (Oxf) 36:102182
43. Wang Z, Ye J, Liu S, Zhang X, Hou Y, Li X, Wang H (2025) Enhanced energy storage capability of hydroxylated BiFeO3/PVDF composites designed by compositionally gradient multilayer structures. J Alloys Compd 1010:177194
44. Dash S, Choudhary RNP, Goswami MN (2017) Enhanced dielectric and ferroelectric properties of PVDF-BiFeO3 composites in 0–3 connectivity. J Alloys Compd 715:29–36
45. Bhattarai MK, Tripathi B, Shweta S, Kumar S, Zuluaga-Gómez CC, Katiyar RK, Weiner BR, Katiyar RS, Morell G (2024) Effective polysulfide control in lithium-sulfur batteries utilizing BiFeO3 nanoparticles. APL Mater. https://doi.org/10.1063/5.0209845/3295166
46. Yadav A, Yadav DK, Choudhary BL, Jakhar N, Jain SK, Tripathi B (2022) Study of dielectric response of BaTiO3/PVA composites for energy storage applications. Mater Today Proc 67:894–899
47. Meena HK, Meena K, Verma R, Jain K, Jain SK, Sharma KB, Tripathi B (2024) Tuning of Optical Properties via Annealing of Bismuth Ferrite ($BiFeO_3$) Thin Films. Open Journal of Composite Materials 14:124–131
48. Geetanjali, Yadav DK, Tripathi B, Verma R (2026) Role of β Phase on Dielectric Response of Bismuth Titanate ($Bi_4Ti_3O_{12}$)/PVDF Nanocomposites. Int J Nanosci. https://doi.org/10.1142/S0219581X26400235